arXiv:1108.1212v1 [math-ph] 4 Aug 2011

# From discrete to continuous models of cell colonies: A measure-theoretic approach

Marco Scianna[*], Andrea Tosin[†], Luigi Preziosi

*Department of Mathematics, Politecnico di Torino*
*Corso Duca degli Abruzzi 24, 10129, Torino, Italy*

## Abstract

This paper deals with the derivation of Eulerian models of cell populations out of a microscopic Lagrangian description of the underlying physical particle system. By looking at the spatial distribution of cells in terms of time-evolving probability measures, rather than at individual cell paths, an ensemble representation of the cell colony is obtained, which can be either discrete or continuous according to the spatial structure of the probability. Remarkably, such an approach does not call for any assumption of continuity of the matter, thus providing consistency to the same modeling framework across all levels of representation. In addition, it is suitable to cope with the often ambiguous translation of microscopic arguments into continuous descriptions. Finally, by grounding cell dynamics on cell-cell interactions, it enables the concept of multiscale dynamics to be introduced and linked to the sensing ability of the cells.

**Keywords:** cell populations, probability measures, discrete vs. continuous descriptions, multiscale dynamics

**Mathematics Subject Classification:** 35Q70, 35Q92, 92C17

## 1 Introduction

Models describing the spatiotemporal patterns of cell populations play a prominent role in Mathematical Biology, as they underlie plenty of different applications: from the formation of vascular plexes (angiogenesis, vasculogenesis) to the growth of cell layers and tumor masses, possibly in interaction with surrounding tissues (cancer invasion). The level of description ranges usually from the microscopic scale of single cells to the macroscopic scale of large cell aggregates and tissues.

Looking at relatively recent contributions (see e.g., [2, 3, 9, 14, 17] and references therein), it appears that more and more importance is being given to nonlocal aspects of cell dynamics. Experimental investigations have indeed demonstrated that a relevant component in cell behavior is the ability of single cells to sense the surroundings and take decisions accordingly, in a non strictly mechanical manner. Apart from phenomenological arguments, at the macroscopic level nonlocal terms are often hard to justify within the classical paradigms of the continuum approach. In fact they generally resort to concepts, such as the sensing neighborhood of cells with related sensing radius, which actually pertain to the length scale of a single cell and are therefore not fully compatible with a macroscopic scale viewpoint. Microscopic models are conceptually more appropriate, however the problem still remains of how to translate microscopic ideas into a representation of the system not necessarily focused on individual cells. Indeed, continuous descriptions

---

[*] M. S. was partially funded by the Italian Ministry of University and Research under a grant on "Math Models of the Interactions between Cells and Environment" and by Fondazione Credito di Risparmio di Torino (CRT) through a "Lagrange Project Fellowship".

[†] A. T. was funded by a post-doctoral research scholarship "Compagnia di San Paolo" awarded by the National Institute for Advanced Mathematics "F. Severi" (INdAM, Italy).

are often useful over discrete agent-based ones, especially in case of large cell colonies, for both reducing the analytical and computational complexity of the representation and recovering the global ensemble dynamics.

Inspired by the methods and models developed for crowd dynamics in [11, 12, 18], in this paper we propose a new approach to the modeling of cell populations, based on measure-theoretic probabilistic tools, which permits a coherent representation of the system at both discrete and continuous scales as well as across intermediate levels. While the mathematical structures used here come to be very close to those firstly proposed in the above-mentioned works on crowds, the probabilistic point of view is instead original and finally makes the difference with respect to more traditional approaches, where the "discrete vs. continuous" dichotomy is referred to the spatial scale at which the system is modeled. In our approach, the underlying physical system (i.e., the cell population) is always regarded as a discrete (granular) one, thus all quantities can be directly referred to the scale of a single cell. However, we admit that the positions of the cells are random variables. The key point is to describe the spatiotemporal evolution of the system by following the probability measure (law) attached to each of these variables rather than the variables themselves. This way we naturally pass from a Lagrangian to an Eulerian description, with the possibility to derive discrete or continuous models from the very same abstract framework by acting on the spatial structure of the probability distribution (atomic or absolutely continuous with respect to Lebesgue, respectively). Since the resulting models are such that the spatial distribution of cells affects the (nonlocal) dynamics of intercellular interactions, it turns out that the discrete or continuous character of the aforesaid probability can be related to the sensing ability of the cells themselves, thus providing quite naturally the concepts of *multiscale dynamics* and *scale of the interactions*.

After the above general presentation, the contents of the paper can now be outlined more precisely. This Introduction is concluded by Section 1.1, which collects the main notations and theoretical notions used in the rest of the paper. In Section 2 the mathematical structures based on time-evolving probability distributions are introduced for modeling cell populations by a measure-theoretic approach. In particular, cell-cell interactions are discussed in some detail, including interactions mediated by a chemical possibly released by the cells themselves for signaling purposes. In Section 3 discrete and continuous models are addressed. A quick literature overview is offered, which shows that many recent microscopic/discrete and macroscopic/continuous models of cell colonies fit formally into our general framework. In addition, the latter can also help explain the links between the two levels of description, provided the convenient point of view of probability distributions is taken. Finally, the continuous version of our nonlocal model is studied in the limit of small sensing radius of the cells and local approximations, in the form of nonlinear degenerate diffusion equations, are derived and critically analyzed. In Section 4 the measure-theoretic tools are further exploited toward a hybrid approach, that introduces the above-mentioned concept of multiscale dynamics. In Section 5 a computational analysis of our method is performed by means of illustrative examples, which visualize the influence of the sensing radius and the sensing ability of the cells on the resulting colony dynamics. Finally, in Section 6 conclusions are drawn and possible developments of the method are outlined. The paper is also equipped with Appendix A, which proposes a conceivable derivation of the probability measure equations out of underlying microscopic dynamics of individual cells.

## 1.1 Notations and background

In this section we quickly review some technical aspects, that will be extensively used in the sequel.

**Variables and nondimensionalization.** We use the space $x \in \mathbb{R}^d$ and the time $t \in [0,\, T_{\max}]$, $T_{\max} > 0$ being a certain final time (possibly $+\infty$), as independent variables. The space dimension $d$ is 1, 2, or 3 for physical purposes.

Throughout the paper, we will implicitly assume that these variables are dimensionless viz. referred to some representative values. Particularly, since a significant quantity is cell motility in free run conditions, the non-dimensionalization of space and time is related to the typical cell

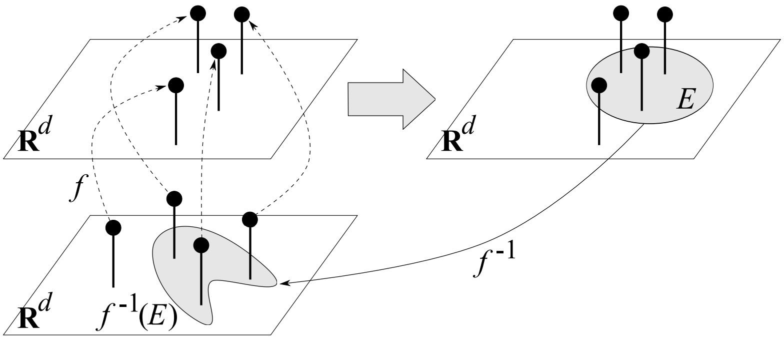

Figure 1: Pictorial representation of the push forward via a mapping $f$ in $\mathbb{R}^d$. After the action of $f$, the measure of a set $E$ is recovered by looking back at its pre-image under $f$. This way, the measure redistribution operated by $f$ is conservative.

speed, say $V$: if space is scaled with respect to a characteristic length $L$ (e.g., the characteristic size of a bounded domain) then time is scaled with respect to $L/V$. As the "spontaneous" motion of a single cell is often regulated by diffusing chemicals, $L$ and $V$ might have a connection with the diffusion dynamics of the latter. For example, $LV$ may be of the same order of magnitude of their diffusion coefficients.

Given the reference values above, we will also tacitly assume that all other dependent variables and parameters are scaled accordingly.

**Functions.** A function $f$ of $t$, $x$ is generically thought of as defined on $[0,\, T_{\max}] \times \mathbb{R}^d$. Instead of the classical $f(t,\, x)$ we prefer the notation $f_t(x)$, which means that we are looking at $f$ as parameterized by time (thus $f_t$, for fixed $t$, is a function defined in $\mathbb{R}^d$). In particular, the subscript $t$ will never stand for time derivative.

The indicator function of a set $A$ is $\mathbb{1}_A$, thus $\mathbb{1}_A(x) = 1$ if $x \in A$, $\mathbb{1}_A(x) = 0$ if $x \notin A$.

The space of real-valued infinitely differentiable functions with compact support in $\mathbb{R}^d$ is $C_c^\infty(\mathbb{R}^d)$.

**Probability measures.** We endow $\mathbb{R}^d$ with the Borel $\sigma$-algebra $\mathscr{B}(\mathbb{R}^d)$. We work with probability measures defined on $\mathscr{B}(\mathbb{R}^d)$ and parameterized by time, that we denote by $\mu_t$. More precisely, if $\mathscr{P}(\mathbb{R}^d)$ is the space of probability measures on $\mathbb{R}^d$ then $\mu_t$ is a mapping $t \mapsto \mathscr{P}(\mathbb{R}^d)$.

The integral on $\mathbb{R}^d$ of a function $f$ with respect to $\mu_t$ will be denoted by $\int_{\mathbb{R}^d} f\, d\mu_t$ or, if it is necessary to specify the variable of integration, by $\int_{\mathbb{R}^d} f(x)\, d\mu_t(x)$.

The push-forward of $\mu_t$ by a Borel-measurable function $f : \mathbb{R}^d \to \mathbb{R}^d$ is a conservative redistribution of $\mu_t$ in $\mathbb{R}^d$, which generates a new probability measure denoted by $f\#\mu_t$ and defined as

$$(f\#\mu_t)(E) := \mu_t(f^{-1}(E)), \quad \forall\, E \in \mathscr{B}(\mathbb{R}^d),$$

see Fig. 1.

**Random variables and stochastic processes.** When dealing with random variables, we consider them as defined on an abstract probability space $(\Omega,\, \mathscr{F},\, P)$ and valued in the measurable space $(\mathbb{R}^d,\, \mathscr{B}(\mathbb{R}^d))$. Here, $\Omega$ is an abstract set (i.e., a set with no special structure), $\mathscr{F}$ is a $\sigma$-algebra of subsets of $\Omega$, and $P$ is a probability measure on $\mathscr{F}$. For stochastic processes, we further assume that they are progressively measurable with respect to a filtration $(\mathscr{F}_t)_{t\in[0,\, T_{\max}]}$.

The expected value of a random variable $X : \Omega \to \mathbb{R}^d$ is denoted $\mathbb{E}[X]$. Depending on the context, it can be computed by one of the following formulas:

$$\mathbb{E}[X] = \int\limits_\Omega X(\omega)\, dP(\omega) = \int\limits_{\mathbb{R}^d} x\, d(X\#P)(x),$$

$X\#P \in \mathscr{P}(\mathbb{R}^d)$ being the law of $X$.

## 2 Modeling cell colonies by time-evolving probability measures

Following the ideas outlined in [21], we model the position of a given cell in the physical space $\mathbb{R}^d$ as a random variable $X_t^i$ valued in the measurable space $(\mathbb{R}^d, \mathscr{B}(\mathbb{R}^d))$. If the total number of cells in the colony is $N$ then $i = 1, \dots, N$. However, instead of looking at the individual paths of the cells, we abstract their spatiotemporal evolution into that of the probability distribution attached to each $X_t^i$. Therefore, the task is to devise a proper evolution model for such a distribution. A practical assumption for reducing the complexity of the problem is that cells within the same population are indistinguishable from one another. This is translated, in mathematical terms, as the $X_t^i$'s being identically distributed: $\mu_t := X_t^i\#P$ is their common law at time $t$, independently of the index $i$ labeling the cell.

The key observation, leading to an equation for $\mu_t$, is that the knowledge of the probability distribution allows one to compute the (average) number of cells contained in a given set $E \subseteq \mathbb{R}^d$ at time $t$. Indeed, let $N_t^E : \Omega \to \mathbb{N}$ be the random variable counting the cells in $E \in \mathscr{B}(\mathbb{R}^d)$ at time $t$, i.e.,

$$N_t^E = \sum_{i=1}^N \mathbb{1}_E(X_t^i).$$

The aforesaid average number can be understood as the expected value of $N_t^E$, which is

$$\mathbb{E}[N_t^E] = \sum_{i=1}^N \int_\Omega \mathbb{1}_E(X_t^i(\omega))\,dP(\omega) = \sum_{i=1}^N \int_{\mathbb{R}^d} \mathbb{1}_E(x)\,d\mu_t(x) = N\mu_t(E). \tag{1}$$

This simple formula matches the intuitive idea that the probability of finding a cell in a given set at a given time is the ratio between the average number (over several repeated experiments) of cells found in that set at that time and the total size of the cell population. $\mathbb{E}[N_t^E]$ can be thought of as the *mass* of the set $E$ at time $t$. In particular, from the relation (1) we infer that the mapping $E \mapsto \mathbb{E}[N_t^E]$ is, for fixed $t$, a measure proportional to $\mu_t$, that we denote by $m_t$. Since $m_t(\mathbb{R}^d) = N\mu_t(\mathbb{R}^d) = N$ is constant in time, i.e., the total mass of the system is conserved, it is coherent to assume that the measure $m_t$ satisfies the conservation law

$$\frac{\partial m_t}{\partial t} + \nabla \cdot (m_t v_t) = 0,$$

where $v_t = v_t(x) \in \mathbb{R}^d$ is a suitable transport velocity. Substituting Eq. (1) gives an analogous evolution equation for the probability $\mu_t$:

$$\frac{\partial \mu_t}{\partial t} + \nabla \cdot (\mu_t v_t) = 0. \tag{2}$$

*Remark* 1. Equation (2) has to be understood in the weak sense of distributions, namely

$$\frac{d}{dt}\int_{\mathbb{R}^d} \psi\,d\mu_t = \int_{\mathbb{R}^d} \nabla\psi \cdot v_t\,d\mu_t, \quad \forall\,\psi \in C_c^\infty(\mathbb{R}^d). \tag{3}$$

The interested reader is referred to [21] for a precise characterization of the concept of solution to such an equation.

## 2.1 Cell-cell interactions

The dynamics of cell colonies are significantly determined by mutual interactions. This is because cells, as living matter, are not passively prone to Newtonian laws of inertia but are able to actively develop behavioral strategies depending on the presence of other neighboring cells and of chemical fields. To some extent, the modeling of cell dynamics can take advantage of certain ideas developed for other systems of interacting living subjects, such as human crowds and groups of animals, see e.g., [10, 11]. Particularly, we borrow the idea that the active behavior of cells, as opposed to the passive one of inert matter, is translated into mathematical models by a direct modeling of the velocity, that cells are able to tune for themselves, rather than of the acceleration.

The following general form of $v_t$, to be inserted in Eq. (2), can be proposed:

$$v_t(x) = \mathcal{T}[c_t](x) + N \int\limits_{\mathbb{R}^d} K(x,\, y)\, d\mu_t(y), \tag{4}$$

where:

- $\mathcal{T}[c_t] : \mathbb{R}^d \to \mathbb{R}^d$ is a taxis-like motion field generated by the spatial distribution of some chemical, whose concentration at time $t$ is $c_t$, that cells are sensitive to. We recall here, among other examples, the cases of chemotaxis, angiogenesis, vasculogenesis. $\mathcal{T}$ is a taxis operator, for instance for chemotaxis it is the spatial gradient, $\mathcal{T}[c_t] \propto \nabla c_t$. This component of the velocity expresses *indirect*, or mediated, interactions among cells (particularly when the chemical is released by cells themselves for signaling purposes like in vasculogenesis).
- $K : \mathbb{R}^d \times \mathbb{R}^d \to \mathbb{R}^d$ is the *interaction kernel*, expressing how a cell in $x$, hereafter called *test cell*, would interact with a neighboring cell in $y$, hereafter called *field cell*. Notice that only linearly additive binary interactions are taken into account in the present framework (see Section 3.1 for further discussions on this issue). This component of the velocity expresses *direct* mean field interactions among cells.

  A typical form of $K$ is as follows:

  $$K(x,\, y) = k(y - x), \tag{5}$$

  with $k : \mathbb{R}^d \to \mathbb{R}^d$, i.e., the interaction between the test cell and a field cell depends on their relative position. When $K$ has this structure, the interaction integral in Eq. (4) can be read as a convolution between $k$ and the measure $\mu_t$:

  $$N \int\limits_{\mathbb{R}^d} k(y - x)\, d\mu_t(y) = N(k * \mu_t)(x).$$

In model (4), direct interactions are nonlocal because the integral over $\mathbb{R}^d$ encompasses both near and far field cells. Indirect interactions may instead be either local or nonlocal, depending on the operator $\mathcal{T}$. In both cases, they may have long-range effects due to the chemical dynamics. We refer the reader to Appendix A for motivating the form (4) of cell velocity starting from microscopic cell dynamics written in terms of the random variables $X_t^i$.

A biologically reasonable assumption is that direct interactions extend over a finite range from the test cell. This is translated, in mathematical terms, by letting the function $K(x,\, \cdot)$ have, for all $x \in \mathbb{R}^d$, compact support, say

$$U_R(x) := \operatorname{supp} K(x,\, \cdot) \subseteq \mathcal{B}_R(x),$$

where $\mathcal{B}_R(x) \subset \mathbb{R}^d$ is the ball centered at $x$ with radius $0 < R < +\infty$. Consequently, the interaction integral in Eq. (4) can be rewritten equivalently as

$$N \int\limits_{U_R(x)} K(x,\, y)\, d\mu_t(y).$$

In the sequel, we will call $R$ the *sensing radius* and $U_R(x)$ the *sensing neighborhood.* Notice that the latter may either coincide or be a proper subset of $\mathcal{B}_R(x)$. In the first case interactions are said to be *isotropic* (i.e., equally expressed all around the test cell), in the second case *anisotropic* (i.e., expressed only when external stimuli due to the presence of field cells come from specific directions).

The chemical concentration can be assumed to obey classical reaction-diffusion dynamics, which implies the following prototypical evolution equation for $c_t$:

$$\frac{\partial c_t}{\partial t} = \nabla \cdot (D \nabla c_t) + \alpha N \mu_t - \gamma c_t, \tag{6}$$

where $D \in \mathbb{R}^{d \times d}$ is the diffusion tensor (symmetric, positive definite), $\alpha \geq 0$ is the rate of autocrine production of the chemical by cells, and $\gamma \geq 0$ is the degradation rate of the chemical in the environment.

*Remark* 2. Equation (6) is meant again in the sense of distributions:

$$\frac{d}{dt} \int\limits_{\mathbb{R}^d} \psi c_t \, dx = \int\limits_{\mathbb{R}^d} \nabla \cdot (D^T \nabla \psi) c_t \, dx + \alpha N \int\limits_{\mathbb{R}^d} \psi \, d\mu_t - \gamma \int\limits_{\mathbb{R}^d} \psi c_t \, dx, \quad \forall \, \psi \in C_c^\infty(\mathbb{R}^d),$$

$D^T \in \mathbb{R}^{d \times d}$ being the transpose of $D$.

By putting Eqs. (2), (4), (6) together, the following Eulerian model is finally obtained:

$$\begin{cases} \dfrac{\partial \mu_t}{\partial t} + \nabla \cdot \left[ \mu_t \left( \mathcal{T}[c_t](x) + N \displaystyle\int\limits_{\mathbb{R}^d} K(x, y) \, d\mu_t(y) \right) \right] = 0 \\ \dfrac{\partial c_t}{\partial t} = \nabla \cdot (D \nabla c_t) + \alpha N \mu_t - \gamma c_t, \end{cases} \tag{7}$$

A qualitative analysis of the initial-value problem associated with model (7), concerning in particular the existence of measure-valued solutions $t \mapsto \mu_t$ and the convergence to them of a properly conceived approximation scheme, is performed in the already cited paper [21], however disregarding the coupling with the chemical field $c_t$. Out of such an analysis, suitable forms of the interaction kernel $K$ are discussed in both the isotropic and anisotropic cases.

## 3 Discrete and continuous cell models

The mathematical structure (7) can take advantage of the measure-theoretic formulation to constitute a paradigm for both discrete and continuous models of cell colonies.

**Discrete cell models.** Discrete cell models are obtained from the assumption that the probability $\mu_t$ is atomic, i.e.,

$$\mu_t = \frac{1}{N} \sum_{h=1}^{N} \delta_{x_h(t)}, \tag{8}$$

where $\mathcal{X}_t := \{x_h(t)\}_{h=1}^N$ is a time-varying set of $N$ points in $\mathbb{R}^d$. This amounts to saying that the random variable $X_t^i$ is a discrete one, uniformly distributed in $\mathcal{X}_t$. In other words, $X_t^i$ takes the values $x_1(t), \ldots, x_N(t)$ each with probability $1/N$. In this case, the mass $m_t$ of a set $E \in \mathscr{B}(\mathbb{R}^d)$ is

$$m_t(E) = N \mu_t(E) = \sum_{h=1}^{N} \delta_{x_h(t)}(E) = \text{card}(E \cap \mathcal{X}_t),$$

i.e., the number of points $x_1(t), \ldots, x_N(t)$ contained in $E$ (counting measure). Notice that, owing to the hypothesis of indistinguishability, it is not possible to associate deterministically the $i$-th cell with its actual position in $\mathbb{R}^d$ at time $t$ (it can be, with equal probability, any of the points in $\mathcal{X}_t$). However, following the time evolution of the set $\mathcal{X}_t$ is enough for an Eulerian description of the cell population as a whole.

Plugging Eq. (8) into Eq. (3) gives

$$\sum_{h=1}^{N} \nabla\psi(x_h(t)) \cdot \frac{dx_h(t)}{dt} = \sum_{h=1}^{N} \nabla\psi(x_h(t)) \cdot v_t(x_h(t)), \quad \forall\, \psi \in C_c^\infty(\mathbb{R}^d),$$

whence $\frac{dx_h}{dt} = v_t(x_h)$ in view of the arbitrariness of $\psi$. Using Eq. (4) for evaluating $v_t(x_h)$ and considering the coupling with Eq. (6) ultimately yields

$$\begin{cases} \dfrac{dx_h}{dt} = \mathcal{T}[c_t](x_h) + \displaystyle\sum_{l=1}^{N} K(x_h,\, x_l), \quad h = 1,\, \dots,\, N \\ \dfrac{\partial c_t}{\partial t} = \nabla \cdot (D\nabla c_t) + \alpha \displaystyle\sum_{l=1}^{N} \delta_{x_l(t)} - \gamma c_t. \end{cases} \tag{9}$$

Model (9) is technically a hybrid instance of model (7), as it is based on a discrete representation of the cell colony within a continuous description of the chemical field.

**Continuous cell models.** Continuous cell models are obtained from the assumption that the probability $\mu_t$ is absolutely continuous with respect to the Lebesgue measure in $\mathbb{R}^d$. Then there exists a nonnegative integrable function $\hat{\rho}_t$ such that

$$d\mu_t = \hat{\rho}_t\, dx, \tag{10}$$

or $\mu_t(E) = \int_E \hat{\rho}_t(x)\, dx$ for all $E \in \mathscr{B}(\mathbb{R}^d)$. In this case, the random variable $X_t^i$ is a continuous one. Furthermore, also the mass $m_t$ is absolutely continuous with respect to the Lebesgue measure, its density being $\rho_t := N\hat{\rho}_t$. The latter can be interpreted as the mass density of the cell population, whence the mass of a set $E \in \mathscr{B}(\mathbb{R}^d)$ is obtained as

$$m_t(E) = N\mu_t(E) = \int\limits_E \rho_t(x)\, dx.$$

By using (10) in Eq. (3), one recognizes the weak form of the conservation law

$$\frac{\partial\hat{\rho}_t}{\partial t} + \nabla \cdot (\hat{\rho}_t v_t) = 0.$$

With the velocity field (4) written for the measure (10):

$$v_t(x) = \mathcal{T}[c_t](x) + N \int\limits_{\mathbb{R}^d} K(x,\, y)\hat{\rho}_t(y)\, dy \tag{11}$$

and coupled with Eq. (6), this gives rise finally to the model

$$\begin{cases} \dfrac{\partial\hat{\rho}_t}{\partial t} + \nabla \cdot \left[\hat{\rho}_t \left(\mathcal{T}[c_t](x) + N \displaystyle\int\limits_{\mathbb{R}^d} K(x,\, y)\hat{\rho}_t(y)\, dy\right)\right] = 0 \\ \dfrac{\partial c_t}{\partial t} = \nabla \cdot (D\nabla c_t) + \alpha N\hat{\rho}_t - \gamma c_t, \end{cases} \tag{12}$$

namely a fully continuous instance of model (7).

## 3.1 Quick overview of some pertinent literature

At this point it is useful to compare the description of cell populations delivered by the measure equation

$$\frac{\partial \mu_t}{\partial t} + N\nabla\cdot\left[\mu_t\int_{\mathbb{R}^d} K(x,\,y)\,d\mu_t(y)\right] = 0 \tag{13}$$

(cf. Eqs. (2), (4) decoupled from chemical dynamics, i.e., with $\mathcal{T} = 0$) with the extensive literature available on the topic. This can indeed contribute to a deeper understanding of our approach, which, as it should be clear from the previous sections and from Appendix A, is conceptually different from taking directly either the microscopic or the macroscopic point of view. As discussed before, a formal comparison is possible with both microscopic/discrete and macroscopic/continuous models. Therefore, for future reference, we explicitly write Eq. (13) with the discrete probability (8):

$$\frac{dx_h}{dt} = \sum_{l=1}^{N} K(x_h,\,x_l), \qquad h = 1,\,\dots,\,N \tag{14}$$

and with the absolutely continuous one (10):

$$\frac{\partial \hat{\rho}_t}{\partial t} + N\nabla\cdot\left[\hat{\rho}_t\int_{\mathbb{R}^d} K(x,\,y)\hat{\rho}_t(y)\,dy\right] = 0. \tag{15}$$

To begin with, it is particularly instructive to examine the paper [13], in which the derivation of models at either scale is discussed through a progressive coarsening of the spatial resolution. Microscopic dynamics are assumed to be ruled by a Langevin's equation of the form

$$\underbrace{m_i\frac{dv_i}{dt}}_{(1)} + \underbrace{\gamma v_i}_{(2)} + \underbrace{\sum_{\substack{j=1\\ j\neq i}}^{N} \gamma_{ij}(v_i^{ij}-v_j^{ij})}_{(3)} = \underbrace{\int_0^t \kappa_m(t-\tau)v_i(\tau)\,d\tau}_{(4)} + \underbrace{\sum_{j=1}^{N} F_{ij}}_{(5)} + \underbrace{f_i(t)}_{(6)}, \tag{16}$$

where $m_i$, $v_i$ are the mass and velocity, respectively, of the $i$-th cell (out of a population of $N$ cells) and the various terms have the following meanings:

(1) is the inertial force acting on the $i$-th cell;

(2) is the (viscous) friction of the $i$-th cell with the outer environment, $\gamma > 0$ being the friction coefficient;

(3) is the (viscous) friction of the $i$-th cell with the surrounding cells, in particular $v_i^{ij}$ is the velocity of the $i$-th cell at the contact point with the $j$-th cell (and similarly for $v_j^{ij}$) and $\gamma_{ij} > 0$ is the cell-cell friction coefficient; notice that this term accounts implicitly for the characteristic size of a cell;

(4) is a memory term, with related memory kernel $\kappa_m$, expressing the tendency of a cell to keep the direction of motion (persistence);

(5) is the resultant of pairwise actions exerted on the $i$-th cell by neighboring cells;

(6) is a zero-mean time-uncorrelated random motion of the $i$-th cell.

Conceivable simplifications of these general dynamics are obtained by neglecting inertia (1, friction-dominated motion), cell-cell friction (3), and persistence memory (4). Up to rescaling the noise as $f_i(t) = \sqrt{2\gamma^2 D}\eta_i(t)$, where $D > 0$ is a random motility coefficient, Eq. (16) takes then the form

$$\frac{dx_i}{dt} = \frac{1}{\gamma}\sum_{j=1}^{N} F_{ij} + \sqrt{2D}\eta_i(t), \tag{17}$$

where $x_i$ is the position of the $i$-th cell (thus $\frac{dx_i}{dt} = v_i$). Equation (17) resembles Eq. (14) but for the noise term, which is indeed possibly meaningless in an averaged representation such as the one delivered by probability measures (cf. Appendix A). Actually, since Eq. (17) is meant to model cell-based microscopic dynamics, its counterpart in our approach is more properly Eq. (26) for the random variables $X_t^i$, with which the analogy is evident if one sets $\mathcal{T} = 0$.

Similar ideas are used also in [15], where an equation of the form (17), though without stochastic noise, is derived under the assumption of friction-dominated dynamics. In this case, the formal comparison is with our discrete equation (14), which however describes actually the evolution of the support $\mathcal{X}_t$ of the probability measure (8).

In order to pass to a macroscopic model, in [13] an intermediate stochastic description by a cellular automaton is adopted, whose evolution rules are inspired by the microscopic model (17). In more detail, the space is partitioned in a number of sites, in each of which cell division and apoptosis at respective rates $\lambda$, $\zeta > 0$ are taken into account, as well as hopping between adjacent sites at rate $\phi > 0$. By further coarsening the spatial resolution, the following equation for the cell density $\rho_t = \rho_t(x)$ is finally obtained:

$$\frac{\partial \rho_t}{\partial t} = \ell^2 \frac{\lambda + \phi}{2d} \Delta \rho_t + [\lambda(1 - \rho_t) - \zeta]\rho_t + \sqrt{2\lambda\rho_t}\eta_t,$$

where $d$ is, like in our setting, the geometric dimension of the spatial domain and $\ell$ is the characteristic size of a cell. The former is a stochastic partial differential equation, which, in the absence of cell duplication and death ($\lambda = \zeta = 0$), gives rise to a linear deterministic local model for cell motion:

$$\frac{\partial \rho_t}{\partial t} = \frac{\ell^2 \phi}{2d} \Delta \rho_t$$

to be compared with the nonlinear local models that we obtain from Eq. (15) in the limit of small sensing radius (cf. Section 3.2).

Other authors [2, 3, 17] take directly a macroscopic point of view, modeling cell dynamics on a phenomenological basis by a conservation law of the form

$$\frac{\partial \rho_t}{\partial t} + \frac{\phi}{R} \nabla \cdot (\rho_t F) = D \Delta \rho_t, \tag{18}$$

where $D > 0$ is the diffusion coefficient showing up at the macroscopic scale as a consequence of random microscopic cell dynamics and $F$ is the total force acting on a cell due to the presence of other surrounding cells. The coefficient $\phi > 0$ is a kind of viscosity of the cellular matter seen as a continuum and $R > 0$ is the sensing radius of the cells. Specifically, $F$ is written as the sum of individual contributions within a sensing neighborhood extending up to a distance $R$ from the cell:

$$F = \alpha \int\limits_{\mathcal{B}_R(x)} \Omega(|y - x|) \frac{y - x}{|y - x|} g(\rho_t(y))\, dy, \tag{19}$$

see also [9]. Notice that $\frac{\phi}{R} F$ is the advection velocity of the cells, to be compared with our Eq. (11) (with $\mathcal{T} = 0$). In particular, if we assume that our interaction kernel is of type (5) with $k$ compactly supported in the ball $\mathcal{B}_R(0)$ then setting $k(z) = \alpha \Omega(z) z / |z|$ and choosing $g(z) = z$ makes Eqs. (15) and (18) formally consistent with one another (but for the linear diffusion term at the right-hand side of Eq. (18), that however we can easily include in our equations as shown in Appendix A). Some comments about the relationships between our model (15) and model (18)-(19) are in order.

- Interactions described by Eq. (19) are, in general, nonlinearly additive whenever the function $g$ is nonlinear. In contrast, our model features linearly additive interactions only. Concerning this, it is worth noticing that nonlinearly additive interactions are technically possible only when the density of cells can be defined. They cannot be straightforwardly extended to the case of more general mass measures (e.g., Dirac measures) because the action of a function $g$ on an abstract measure is typically not defined.

- Model (18)-(19) relies on the concept of sensing radius of the cells, which is however not rigorously justifiable at the macroscopic scale because it pertains intrinsically to a microscopic length scale. Instead, with our approach it is fully acceptable also in a continuous context, since "continuous" refers here to the space structure of the probability distribution of cells, the underlying physical system remaining discrete and microscopic.

Finally, we want to mention the chemotaxis model proposed in [14], which describes cells as a continuum with density $\rho_t$ subject to interactions mediated by a chemical factor $c_t$:

$$\begin{cases} \dfrac{\partial \rho_t}{\partial t} + \nabla \cdot (\chi \rho_t \mathring{\nabla}_r c_t) = D_\rho \Delta \rho_t \\ \dfrac{\partial c_t}{\partial t} = D_c \Delta c_t + \alpha \rho_t - \gamma c_t. \end{cases}$$

Here, $\mathring{\nabla}_r$ denotes a nonlocal gradient sensed at a distance $r > 0$ from the cell:

$$\mathring{\nabla}_r c_t(x) = \frac{d}{r\,|\partial \mathcal{B}_1(0)|} \int\limits_{\partial \mathcal{B}_1(0)} \sigma c_t(x + \sigma r)\, d\sigma.$$

These equations can be duly compared with our continuous model (12) by setting $K = 0$ (and including the random motion of cells as explained in Appendix A). In particular, we notice that the nonlocal gradient may be a valuable hint for modeling the taxis operator $\mathcal{T}$, considering that, for the same reasons discussed above, our framework enables us to handle rigorously the non-locality introduced by the parameter $r$ as a microscopic feature of individual cells.

## 3.2 Nonlocal vs. local continuous models

Unlike those presented in Section 3.1, several other models of population dynamics are formulated assuming local (namely, pointwise) interactions, usually by means of nonlinear advection-diffusion equations at a continuous level [4, 5, 23]. In this section we investigate which kind of local continuous cell models can be obtained from the nonlocal equation (15) (cf. also [22]) under the assumption of small sensing radius. In particular, we discuss suitable analytical forms of such models in view of the locally dominant cell behavior (attraction or repulsion). For the sake of simplicity, we confine ourselves to the one-dimensional setting ($d = 1$). We consider interactions depending on the relative position of the cells (cf. Eq. (5)), addressing separately the isotropic and anisotropic case.

### 3.2.1 Isotropic interactions

The sensing neighborhood of the point $x$ is $U_R(x) = (x - R,\, x + R)$, hence the velocity takes the form

$$v_t(x) = N \int\limits_{x-R}^{x+R} k(y - x) \hat{\rho}_t(y)\, dy. \tag{20}$$

Notice that, in the interaction integral, it results $|y - x| \leq R$. If $R$ is small and we assume that $k$, $\hat{\rho}_t$ are sufficiently smooth, we can expand the first one about zero and the second one about $x$ as

$$\begin{aligned} k(z) &= k(0) + k'(0)z + \frac{1}{2}k''(0)z^2 + \frac{1}{6}k'''(0)z^3 + \frac{1}{24}k^{IV}(0)z^4 + o(z^4) \\ \hat{\rho}_t(y) &= \hat{\rho}_t(x) + \frac{\partial \hat{\rho}_t}{\partial x}(x)(y - x) + \frac{1}{2}\frac{\partial^2 \hat{\rho}_t}{\partial x^2}(x)(y - x)^2 + \frac{1}{6}\frac{\partial^3 \hat{\rho}_t}{\partial x^3}(x)(y - x)^3 \\ &\quad + \frac{1}{24}\frac{\partial^4 \hat{\rho}_t}{\partial x^4}(x)(y - x)^4 + o((y - x)^4), \end{aligned} \tag{21}$$

whence

$$
\begin{aligned}
k(y-x)\hat{\rho}_t(y) = k(0)\hat{\rho}_t(x) &+ \left(k(0)\frac{\partial\hat{\rho}_t}{\partial x}(x) + k'(0)\hat{\rho}_t(x)\right)(y-x) \\
&+ \left(\frac{1}{2}k(0)\frac{\partial^2\hat{\rho}_t}{\partial x^2}(x) + k'(0)\frac{\partial\hat{\rho}_t}{\partial x}(x) + \frac{1}{2}k''(0)\hat{\rho}_t(x)\right)(y-x)^2 \\
&+ \left(\frac{1}{6}k(0)\frac{\partial^3\hat{\rho}_t}{\partial x^3}(x) + \frac{1}{2}k'(0)\frac{\partial^2\hat{\rho}_t}{\partial x^2}(x) + \frac{1}{2}k''(0)\frac{\partial\hat{\rho}_t}{\partial x}(x)\right. \\
&\qquad \left. + \frac{1}{6}k'''(0)\hat{\rho}_t(x)\right)(y-x)^3 \\
&+ \left(\frac{1}{24}k(0)\frac{\partial^4\hat{\rho}_t}{\partial x^4}(x) + \frac{1}{6}k'(0)\frac{\partial^3\hat{\rho}_t}{\partial x^3}(x) + \frac{1}{4}k''(0)\frac{\partial^2\hat{\rho}_t}{\partial x^2}(x)\right. \\
&\qquad \left. + \frac{1}{6}k'''(0)\frac{\partial\hat{\rho}_t}{\partial x}(x) + \frac{1}{24}k^{IV}(0)\hat{\rho}_t(x)\right)(y-x)^4 + o((y-x)^4).
\end{aligned}
$$

Now, since

$$
\int\limits_{x-R}^{x+R}(y-x)^n\,dy = \begin{cases} 0 & n \text{ odd} \\ \dfrac{2R^{n+1}}{n+1} & n \text{ even,} \end{cases}
$$

we obtain from Eq. (20), neglecting the term $o((y-x)^4)$,

$$
v_t(x) = C_0\hat{\rho}_t(x) + C_1\frac{\partial\hat{\rho}_t}{\partial x}(x) + C_2\frac{\partial^2\hat{\rho}_t}{\partial x^2}(x) + C_3\frac{\partial^3\hat{\rho}_t}{\partial x^3}(x) + C_4\frac{\partial^4\hat{\rho}_t}{\partial x^4}(x), \tag{22}
$$

where the coefficients $C_0, \ldots, C_4$ are

$$
\begin{aligned}
C_0 &= \left(2k(0) + \frac{1}{3}k''(0)R^2 + \frac{1}{60}k^{IV}(0)R^4\right)NR \\
C_1 &= \left(\frac{2}{3}k'(0) + \frac{1}{15}k'''(0)R^2\right)NR^3 \\
C_2 &= \left(\frac{1}{3}k(0) + \frac{1}{10}k''(0)R^2\right)NR^3 \\
C_3 &= \frac{1}{15}k'(0)NR^5 \\
C_4 &= \frac{1}{60}k(0)NR^5.
\end{aligned}
$$

We can further specialize them by introducing the following hypotheses on $k$:

**(H1)** $k(0) = 0$, for excluding self-interactions

**(H2)** $k(-z) = -k(z)$, radial isotropic interactions

which imply that even-order derivatives of $k$ vanish in zero. Consequently:

$$
\begin{aligned}
C_0 &= C_2 = C_4 = 0 \\
C_1 &= \left(\frac{2}{3}k'(0) + \frac{1}{15}k'''(0)R^2\right)NR^3 \\
C_3 &= \frac{1}{15}k'(0)NR^5,
\end{aligned}
$$

hence Eq. (15) is finally approximated as

$$
\frac{\partial\hat{\rho}_t}{\partial t} = -\left[C_1\frac{\partial}{\partial x}\left(\hat{\rho}_t\frac{\partial\hat{\rho}_t}{\partial x}\right) + C_3\frac{\partial}{\partial x}\left(\hat{\rho}_t\frac{\partial^3\hat{\rho}_t}{\partial x^3}\right)\right]. \tag{23}
$$

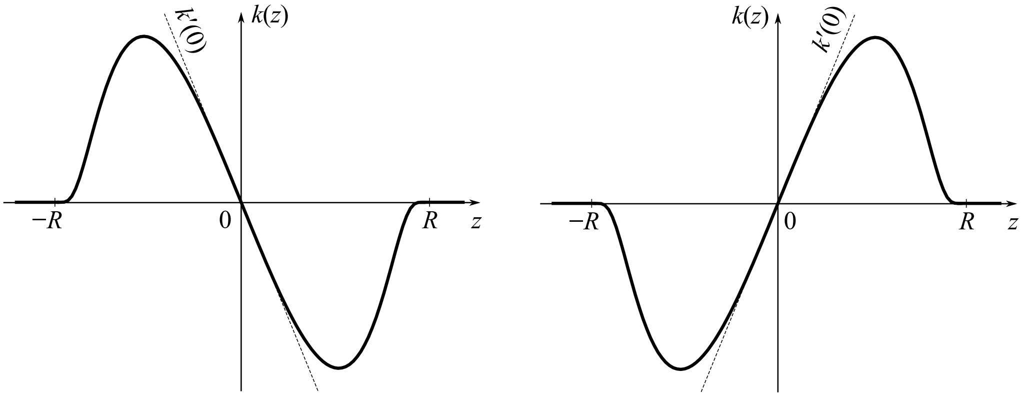

Figure 2: Examples of interaction kernels $k$ (cf. Eq. (5)) for repulsion (left) and attraction (right), with sensing radius $R$. In the first case, field cells located in a left neighborhood of the origin make the test cell in $z = 0$ move preferentially to the right, whereas those located in a right neighborhood make it move preferentially to the left. This is repulsion from populated areas. In the second case, the behavior of the test cell is the opposite, implying attraction toward populated areas.

By introducing the rescaled space $x^* := R^{-1}x$ and time $t^* := |C_1|\,R^{-2}t$ and redefining $\hat{\rho}_t(x) = \hat{\rho}_{|C_1|^{-1}R^2t^*}(Rx^*) =: \hat{\rho}^*_{t^*}(x^*)$, we restate Eq. (23) as

$$\frac{\partial\hat{\rho}^*_{t^*}}{\partial t^*} = -\left[\operatorname{sign}(C_1)\frac{\partial}{\partial x^*}\left(\hat{\rho}^*_{t^*}\frac{\partial\hat{\rho}^*_{t^*}}{\partial x^*}\right) + \frac{C_3}{R^2\,|C_1|}\frac{\partial}{\partial x^*}\left(\hat{\rho}^*_{t^*}\frac{\partial^3\hat{\rho}^*_{t^*}}{\partial {x^*}^3}\right)\right].$$

In the approximation $C_1 = \frac{2}{3}k'(0)NR^3$, which holds for small $R$, it results $\operatorname{sign}(C_1) = \operatorname{sign}(k'(0))$ and $-\frac{C_3}{R^2|C_1|} = -\frac{1}{10}\operatorname{sign}(k'(0))$, thus we ultimately get

$$\frac{\partial\hat{\rho}^*_{t^*}}{\partial t^*} = -\operatorname{sign}(k'(0))\left[\frac{\partial}{\partial x^*}\left(\hat{\rho}^*_{t^*}\frac{\partial\hat{\rho}^*_{t^*}}{\partial x^*}\right) + \frac{1}{10}\frac{\partial}{\partial x^*}\left(\hat{\rho}^*_{t^*}\frac{\partial^3\hat{\rho}^*_{t^*}}{\partial {x^*}^3}\right)\right].$$

This equation combines second and fourth-order nonlinear degenerate diffusion. Its character is strongly determined by the sign of $k'(0)$, in particular we can distinguish the following cases:

- If $k'(0) < 0$ then $\operatorname{sign}(k'(0)) = -1$, which implies that second-order diffusion is the classical forward one, whereas fourth-order diffusion gives the equation a backward character to the leading order. Since backward diffusion equations are ill-posed, especially in terms of continuous dependence of their solutions on the data, when $k'(0) < 0$ it is advisable to stop the expansions (21) at the second order, so as to obtain a well-behaved diffusive local model of the form
$$\frac{\partial\hat{\rho}^*_{t^*}}{\partial t^*} = \frac{\partial}{\partial x^*}\left(\hat{\rho}^*_{t^*}\frac{\partial\hat{\rho}^*_{t^*}}{\partial x^*}\right).$$
Notice that this is consistent with the fact that $k'(0) < 0$ describes a locally repulsive (disaggregating) behavior of the cells (see Fig. 2, left).

- If $k'(0) > 0$ then the picture is the opposite to the previous one. Now $\operatorname{sign}(k'(0)) = 1$, thus second-order diffusion is backward and expansions (21) up to the fourth-order are necessary in order to obtain a formally well-behaved model at the leading order:
$$\frac{\partial\hat{\rho}^*_{t^*}}{\partial t^*} = -\frac{\partial}{\partial x^*}\left(\hat{\rho}^*_{t^*}\frac{\partial\hat{\rho}^*_{t^*}}{\partial x^*}\right) - \frac{1}{10}\frac{\partial}{\partial x^*}\left(\hat{\rho}^*_{t^*}\frac{\partial^3\hat{\rho}^*_{t^*}}{\partial {x^*}^3}\right).$$
Again, this is consistent with the fact that $k'(0) > 0$ describes a locally attractive (aggregating) behavior of the cells (see Fig. 2, right).

### 3.2.2 Anisotropic interactions

In one space dimension, the prototypes of anisotropic sensing neighborhood are the half intervals $U_R(x) = (x,\, x+R)$ and $U_R(x) = (x-R,\, x)$. In this case, the coupling with the chemical dynamics can be exploited for determining the local orientation of $U_R$. For instance, the latter can be chosen in the direction of the taxis motion field in order to reproduce cell polarization. Hence the above alternatives apply for $\mathcal{T}[c_t](x) \geq 0$ and $\mathcal{T}[c_t](x) \leq 0$, respectively. If $\mathcal{T}[c_t]$ changes sign then $U_R$ will not be the same for all points $x$.

For illustrative purposes, in this discussion we fix $U_R(x) = (x,\, x+R)$. After performing the same expansions as in Eq. (21), we observe that now

$$\int\limits_x^{x+R} (y-x)^n \, dy = \frac{R^{n+1}}{n+1},$$

thus the new coefficients $C_0,\, \dots,\, C_4$ to be used in Eq. (22) are:

$$\begin{aligned}
C_0 &= \left( k(0) + \frac{1}{2}k'(0)R + \frac{1}{6}k''(0)R^2 + \frac{1}{24}k'''(0)R^3 + \frac{1}{120}k^{IV}(0)R^4 \right) NR \\
C_1 &= \left( \frac{1}{2}k(0) + \frac{1}{3}k'(0)R + \frac{1}{8}k''(0)R^2 + \frac{1}{30}k'''(0)R^3 \right) NR^2 \\
C_2 &= \left( \frac{1}{6}k(0) + \frac{1}{8}k'(0)R + \frac{1}{20}k''(0)R^2 \right) NR^3 \\
C_3 &= \left( \frac{1}{24}k(0) + \frac{1}{30}k'(0)R \right) NR^4 \\
C_4 &= \frac{1}{120}k(0)NR^5.
\end{aligned}$$

Imposing that $k$ satisfies hypotheses (H1), (H2) yields again that, in the above general expressions, $k(0)$ and all even-order derivatives of $k$ computed in zero vanish. Nevertheless, this time all coefficients of the even-order derivatives of $\hat{\rho}_t$ in Eq. (22) do not vanish because of anisotropy:

$$\begin{aligned}
C_0 &= \frac{1}{2}\left( k'(0) + \frac{1}{12}k'''(0)R^2 \right) NR^2 \\
C_1 &= \frac{1}{3}\left( k'(0) + \frac{1}{10}k'''(0)R^2 \right) NR^3 \\
C_2 &= \frac{1}{8}k'(0)NR^4 \\
C_3 &= \frac{1}{30}k'(0)NR^5 \\
C_4 &= 0.
\end{aligned}$$

Correspondingly, the local equation obtained for the density is

$$\frac{\partial \hat{\rho}_t}{\partial t} + C_0 \frac{\partial}{\partial x}(\hat{\rho}_t^2) = -\left[ C_1 \frac{\partial}{\partial x}\left( \hat{\rho}_t \frac{\partial \hat{\rho}_t}{\partial x} \right) + C_2 \frac{\partial}{\partial x}\left( \hat{\rho}_t \frac{\partial^2 \hat{\rho}_t}{\partial x^2} \right) + C_3 \frac{\partial}{\partial x}\left( \hat{\rho}_t \frac{\partial^3 \hat{\rho}_t}{\partial x^3} \right) \right],$$

which, after rescaling space, time, and density as in Section 3.2.1, reads

$$\begin{aligned}
\frac{\partial \hat{\rho}^*_{t^*}}{\partial t^*} + \frac{3}{2}\,\mathrm{sign}\,(k'(0)) \frac{\partial}{\partial x^*}(\hat{\rho}^{*2}_{t^*}) = -\,\mathrm{sign}\,(k'(0)) \Bigg[ & \frac{\partial}{\partial x^*}\left( \hat{\rho}^*_{t^*} \frac{\partial \hat{\rho}^*_{t^*}}{\partial x^*} \right) + \frac{3}{8}\frac{\partial}{\partial x^*}\left( \hat{\rho}^*_{t^*} \frac{\partial^2 \hat{\rho}^*_{t^*}}{\partial x^{*2}} \right) \\
& + \frac{1}{10}\frac{\partial}{\partial x^*}\left( \hat{\rho}^*_{t^*} \frac{\partial^3 \hat{\rho}^*_{t^*}}{\partial x^{*3}} \right) \Bigg].
\end{aligned}$$

Notice the appearance of the odd-order terms $\partial_{x^*}(\hat{\rho}_{t^*}^{*2})$ at the left-hand side and $\partial_{x^*}(\hat{\rho}_{t^*}^{*}\partial_{x^*}^{2}\hat{\rho}_{t^*}^{*})$ at the right-hand side, which are symptomatic of the anisotropy of the interactions. Once again, the sign of the highest-order derivatives, and consequently the appropriate order of the expansions (21), depends on the sign of $k'(0)$, namely on the local character of the interactions. Considerations analogous to those developed in Section 3.2.1 can therefore be proposed:

- If $k'(0) < 0$ (repulsive or disaggregating interactions) then a second-order expansion is convenient to obtain a formally well-behaved local model:

$$\frac{\partial\hat{\rho}_{t^*}^{*}}{\partial t^*} - \frac{3}{2}\frac{\partial}{\partial x^*}(\hat{\rho}_{t^*}^{*2}) = \frac{\partial}{\partial x^*}\left(\hat{\rho}_{t^*}^{*}\frac{\partial\hat{\rho}_{t^*}^{*}}{\partial x^*}\right).$$

- If $k'(0) > 0$ (attractive or aggregating interactions) then a fourth-order expansion is necessary in order to compensate for the resulting backward second-order diffusion:

$$\frac{\partial\hat{\rho}_{t^*}^{*}}{\partial t^*} + \frac{3}{2}\frac{\partial}{\partial x^*}(\hat{\rho}_{t^*}^{*2}) = -\frac{\partial}{\partial x^*}\left(\hat{\rho}_{t^*}^{*}\frac{\partial\hat{\rho}_{t^*}^{*}}{\partial x^*}\right) - \frac{3}{8}\frac{\partial}{\partial x^*}\left(\hat{\rho}_{t^*}^{*}\frac{\partial^2\hat{\rho}_{t^*}^{*}}{\partial x^{*2}}\right) - \frac{1}{10}\frac{\partial}{\partial x^*}\left(\hat{\rho}_{t^*}^{*}\frac{\partial^3\hat{\rho}_{t^*}^{*}}{\partial x^{*3}}\right).$$

# 4 Hybrid approach for multiscale dynamics

The measure-theoretic formulation of model (7) can be further exploited to come to a hybrid approach, in which discrete and continuous representations of the *same* cell population coexist and complement each other. Technically, this amounts to expressing the probability $\mu_t$ as a combination of an atomic and an absolutely continuous part:

$$\mu_t = (1-u)\frac{1}{N}\sum_{h=1}^{N}\delta_{x_h(t)} + u\hat{\rho}_t\mathcal{L}^d, \tag{24}$$

where $\mathcal{L}^d$ denotes the Lebesgue measure in $\mathbb{R}^d$ and $u \in [0,\,1]$ is a parameter. The purely discrete and continuous cases, discussed in Section 3, can be recovered for $u = 0$ and $u = 1$, respectively; in addition, a full range of intermediate representations is now accessible for $0 < u < 1$.

It is worth stressing that when $u \neq 0,\,1$ neither the sole set of points $\mathcal{X}_t = \{x_h(t)\}_{h=1}^{N}$ nor the sole density $\hat{\rho}_t$ provides the actual space distribution of the cells. According to Eq. (24), the complete picture results instead from a $u$-weighted joint contribution of the twos. In fact, the number of cells contained in a set $E \in \mathscr{B}(\mathbb{R}^d)$ at time $t$ is

$$m_t(E) = (1-u)\,\mathrm{card}(E\cap\mathcal{X}_t) + uN\int_E \hat{\rho}_t(x)\,dx,$$

thus for $u \neq 0$ there might be a nonzero probability of finding a cell in a set $E$ which does not contain any of the points of $\mathcal{X}_t$, whereas for $u \neq 1$ there might be a nonzero probability of finding a cell in a set $E$ where the density $\hat{\rho}_t$ is zero.

With the measure (24) the velocity field (4) takes the form

$$v_t(x) = \mathcal{T}[c_t](x) + (1-u)\sum_{h=1}^{N}K(x,\,x_h(t)) + uN\int_{\mathbb{R}^d}K(x,\,y)\hat{\rho}_t(y)\,dy, \tag{25}$$

which shows that at every point $x \in \mathbb{R}^d$ direct interactions depend simultaneously on the discrete and continuous spatial distribution of the cells.

From the modeling viewpoint, this hybrid approach can be given various, possibly complementary, interpretations. In the following we critically discuss some of them, having in mind the specific application to cell populations understood as living complex systems. As a general fact, we notice that such an approach is different from other hybrid approaches proposed in the literature,

Table 1: Parameters of the model used for the numerical tests of Section 5.

| Parameter | Symbol | Value | |
|---|---|---|---|
| | | Fig. 3 | Fig. 4 |
| Number of cells | $N$ | 25 | |
| Sensing radius | $R$ | 0.3 | 0.6 |
| Cell sensitivity/scale of interactions | $u$ | 0, 0.1, 0.9, 1 | |
| Final time | $T_{\max}$ | 20 | |

in which the discrete and continuous representations refer to distinct parts of the system [8, 19] in a spirit similar to model (9). Here, it is the spatial distribution of one single cell population that is represented at an intermediate level in probabilistic terms.

A first way of understanding the hybrid representation (24) is as a multiscale coupling between the "microscopic" scale of the set $\mathcal{X}_t$ and the "macroscopic" scale of the density $\hat{\rho}_t$, with $u$ playing the role of an interpolation parameter. This interpretation is brought from the multiscale model of crowd dynamics proposed in [12], also based on a measure-theoretic approach to the conservation law (2).

A different point of view, that we promote here, is instead not directly concerned with the above space scale dichotomy. As already stressed, the modeling structures presented in Section 2 refer to an intrinsically microscopic observation of the cell colony, with cell trajectories however blurred into the probability distribution $\mu_t$. Hence, the hybrid approach concerns the representation of the space distribution of cells as an abstract mathematical object, the look at the underlying particle system remaining an individual-based one. In particular, according to Eq. (25), a more discrete or continuous probability distribution influences the outcome of direct interactions among cells. In this sense, it is possibly appropriate to speak of *multiscale dynamics* based on the *scale of the interactions*. The parameter $u$ can then be related to a *sensing ability* of the cells. A value of $u$ close to 0 (discrete representation) may characterize a population in which cells sense precisely other surrounding cells, whereas a value of $u$ close to 1 (continuous representation) denotes a colony of cells that generically feel each other as a whole. This concept will be further discussed and clarified in the next Section 5.

# 5 Numerical tests

In this section, we use numerical simulations for exemplifying various dynamical scenarios generated by the presented model according to different representations of the cell distribution. In order to focus genuinely on the effects of multiscale dynamics, we disregard the coupling with diffusible chemicals, namely we rest on Eq. (13) with the measure $\mu_t$ given by Eq. (24).

Two-dimensional ($d = 2$) simulations are produced by means of a modification of the numerical scheme developed in [12] (cf. also [18, 21] for error and convergence analysis), specifically designed for the measure-theoretic framework with hybrid $\mu_t$. The simulation setting is as follows (cf. Table 1 for a summary of the parameters). The spatial domain is $\Omega = [0, 4] \times [0, 4]$, with an initial distribution of $N = 25$ cells compactly supported in the sub-domain $\Omega_0 = [1, 3] \times [1, 3]$. In more detail, the atoms and the density of the measure (24) at time $t = 0$ are chosen, respectively, as:

$$x_h(0) = \left(\frac{1+h_1}{2},\, \frac{1+h_2}{2}\right), \qquad h_1,\, h_2 = 1,\, \dots,\, 5$$

$$\hat{\rho}_0(x) = \frac{1}{4}\mathbb{1}_{\Omega_0}(x),$$

hence the discrete and continuous parts of the distribution are initially uniform in $\Omega_0$. We model *aggregation* dynamics using an interaction kernel $K$ of the form (5), with $k(z) = z\mathbb{1}_{\mathcal{B}_R(0)}(z)$, resulting in

$$K(x,\, y) = (y - x)\mathbb{1}_{\mathcal{B}_R(x)}(y).$$

Cell-cell interactions are therefore isotropic. We consider two possible values of the sensing radius, $R = 0.3$ and $R = 0.6$, respectively.

Figure 3 refers to the case $R = 0.3$ for different cell sensing abilities, $u = 0$, 0.1, 0.9, 1. In all cases, only partial aggregation of the colony occurs, indeed the final configuration consists in multiple isolated clusters. However, an important difference is immediately seen between the two limit cases $u = 0$ (discrete dynamics) and $u = 1$ (continuous dynamics). In the former, the extremely localized cell sensitivity makes the starting configuration a steady one: because the sensing radius is smaller than the initial intercellular distance, individual atoms do not aggregate. In the latter, the distributed cell sensitivity (which means that the test cell may feel, within its sensing neighborhood, the presence/influence of the surrounding field cells besides their exact position) triggers instead aggregation, leading to the formation of 9 main clusters interspersed with 4 secondary ones. In addition, shadows of additional 4, even less relevant, clusters appear in correspondence of the corners of the original distribution.

Adding a small continuous contribution to the discrete setting ($u = 0.1$, so that 10% of the distribution is continuous and 90% is discrete) changes dramatically the dynamics with respect to the purely discrete case. Most of the mass now concentrates in 4 clusters, including all atoms of the hybrid measure $\mu_t$; a secondary cluster is formed in the middle, however it does not contain atoms. This is due to the fact that purely discrete dynamics are “fragile”, because they strongly depend on the precise locations of the cells. An even small uncertainty in the initial cell distribution, implying a mild spatially continuous component of the measure $\mu_t$, can in fact result in qualitatively very different results.

Conversely, adding a small discrete contribution to the continuous setting ($u = 0.9$, so that 90% of the distribution is continuous and 10% is discrete) does not appreciably perturb the dynamics with respect to the purely continuous case. The same 9 main clusters appear, where all atoms tend to concentrate, again interspersed with 4 secondary clusters without atoms. Actually, in the proposed simulation, at the final time a single atom remains trapped in the upper-right corner of the original distribution, however it corresponds only to a probability of $(1 - u)/N = 0.004$ of finding a cell there (in terms of mass, 10% of the average total mass of the colony).

From the above-described realizations, we can infer that purely continuous dynamics are much more stable to discrete perturbations than purely discrete ones are to continuous perturbations. This is confirmed also by simulations with different values of $u$, for instance $u = 0.7$ (not shown). Nevertheless, by further decreasing $u$ the granularity of the distribution begins to modify the continuous dynamics, indeed the aforesaid 9 main clusters switch to 4 main plus 1 secondary cluster for $u = 0.1$.

Figure 4 shows similar numerical experiments with $R = 0.6$. In this case, the final configuration of the cell distribution is a single cluster for all values of $u$, meaning that the sensing radius is sufficiently large for a full aggregation of the colony to always take place. However, the snapshots at intermediate times display different transient dynamics of aggregation, confirming again the fragility of the purely discrete ones as opposed to the robustness of the purely continuous ones.

# 6 Discussion

In this paper we have introduced a mathematical method, based on conservation laws and measure theory, which is able to describe the spatiotemporal dynamics of cell populations. The proposed approach is intended to cope with the difficulty of providing an Eulerian ensemble representation of cell colonies starting from a Lagrangian individual characterization of a microscopic test entity. More technically, the method consists in modeling cell positions in the physical space as random variables and then in looking at the evolution of their probability distribution (law) rather than at that of the random variables themselves. This way, the underlying physical system is always regarded as a microscopic granular one but its Eulerian representation can be either discrete or continuous according to the specific structure of the probability.

In our opinion, this method offers several conceptual advantages over classical microscopic and macroscopic models. First, it enables one to transfer unambiguously microscopic concepts into

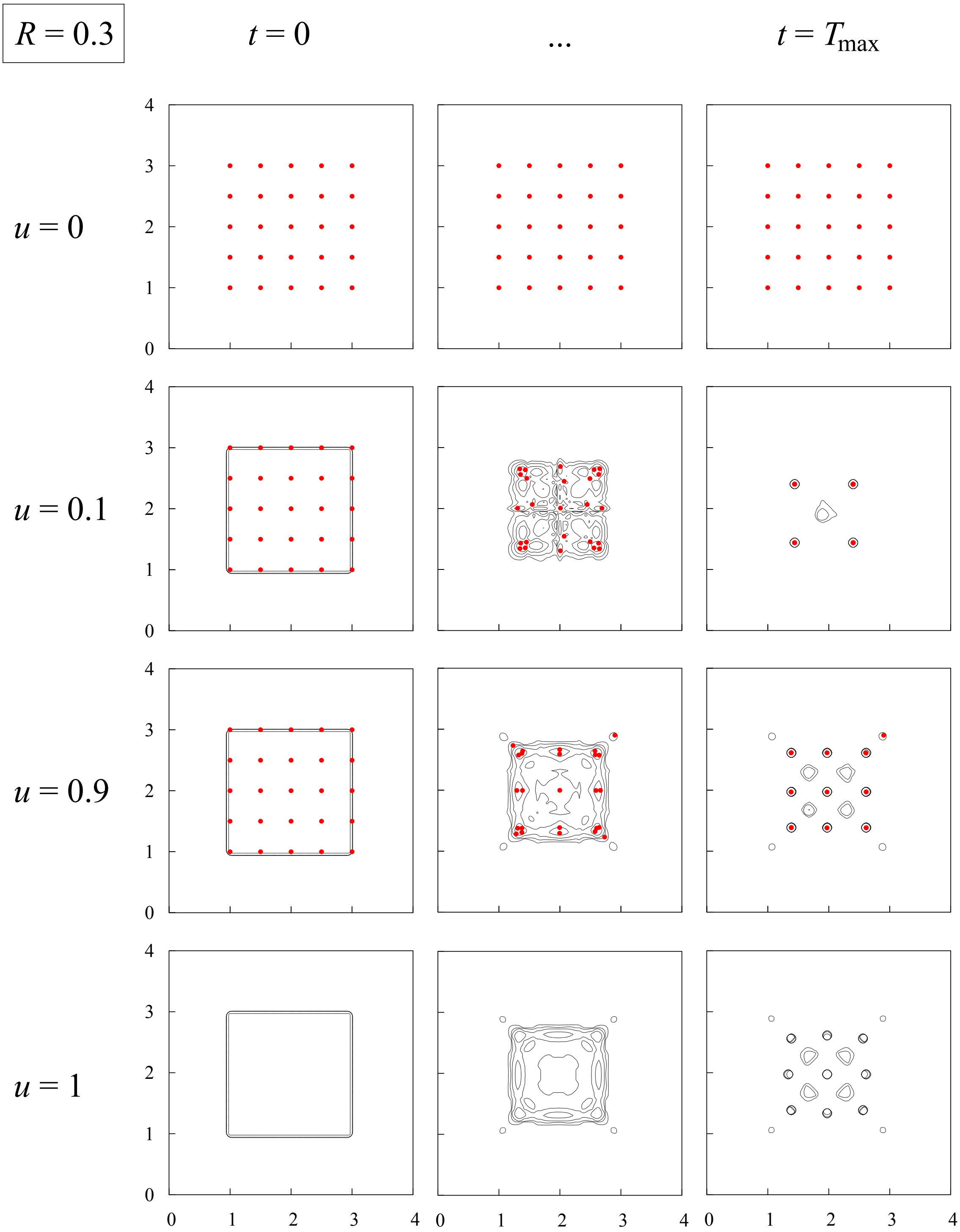

Figure 3: Multiscale dynamics of aggregation with sensing radius $R = 0.3$. In each plot, the atoms $x_h(t)$ and the level curves of the density $\hat{\rho}_t$ are shown.

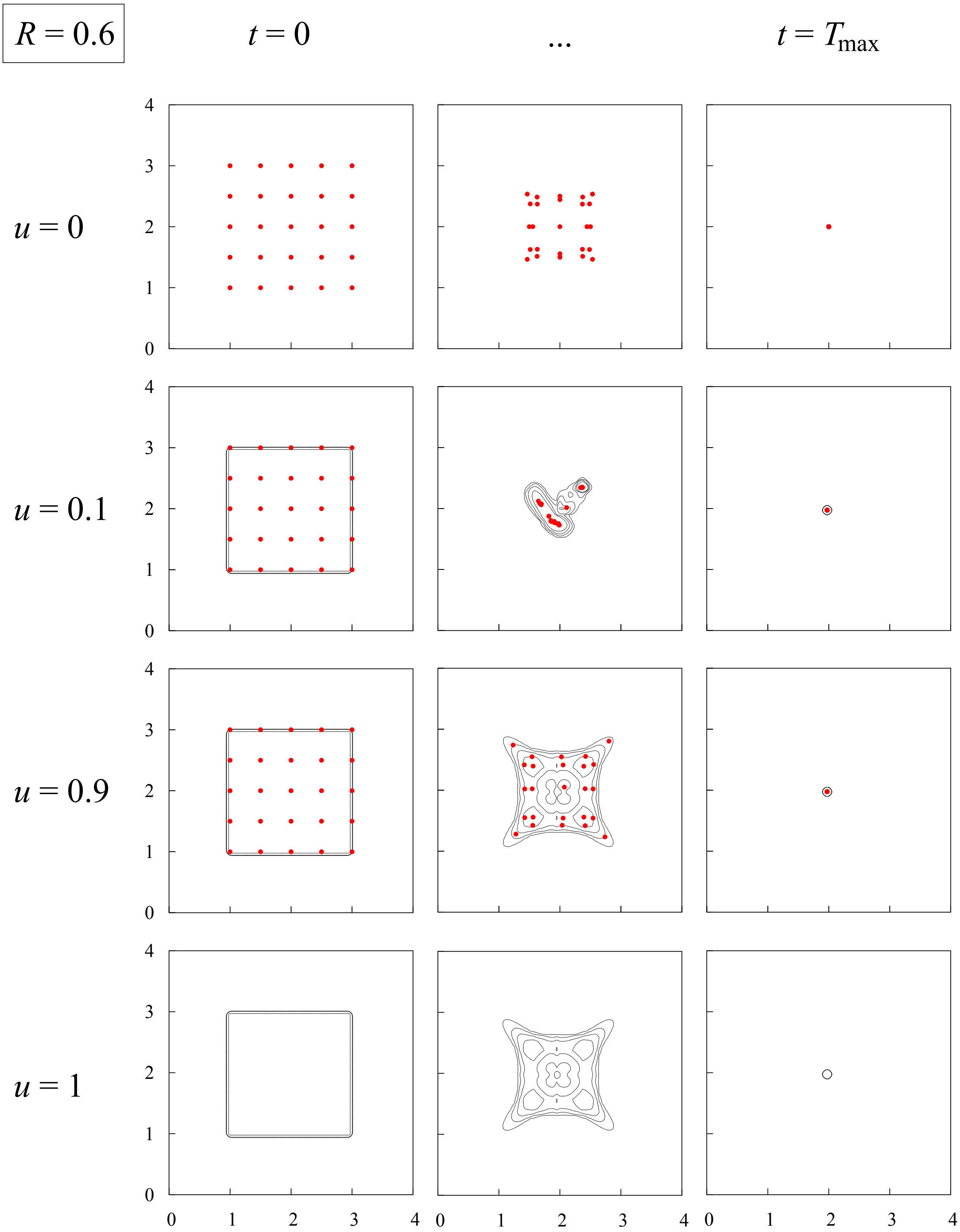

Figure 4: Multiscale dynamics of aggregation with sensing radius $R = 0.6$. In each plot, the atoms $x_h(t)$ and the level curves of the density $\hat{\rho}_t$ are shown.

a spatially continuous description of the cell distribution. This includes, for instance, sensitivity to chemical fields and to other cells within proper neighborhoods. Secondly, in order to obtain a global representation not necessarily focused on individual entities, our approach does not force the assumption that a cell population is a continuous matter. This makes the method suitable to describe both large colonies and small aggregates, for which the limit of an infinite number of cells may not be acceptable. Finally, it permits to embed rigorously the intrinsic granularity (discreteness) of cell populations into a continuous distribution, giving rise to multiscale dynamics that can be linked to the sensing ability expressed by the cells.

In short, the key idea of the method consists in a change of viewpoint: from the physical positions of the cells to the probability measure attached to them. It is worth noticing that, once the latter is available, all important information on the system, such as mass distribution and spatial patterns, is directly recoverable without going back to the detail of the aforesaid random variables. Therefore, the latter mainly serve as conceptual tools for deducing coherently a transport equation of the probability law.

Illustrative simulations have shown nontrivial consequences of the multiscale dynamics on the predicted pattern formation, thus implying that the sensing ability of the cells and the related scale of their mutual interactions are crucial aspects that our framework can include. For this reason, we expect our method to give an interesting contribution in the development of multiscale approaches to the modeling of cell phenomena, particularly in those problems in which the interplay between discrete and continuous descriptions can be linked to different abilities and functions of the cells.

# A From microscopic dynamics to an Eulerian representation of cell colonies

Model (2)-(4) was derived mainly heuristically. This appendix aims at motivating it starting from the level of individual-based dynamics.

The hallmark of the method we are going to apply is that the total number $N$ of cells, though arbitrarily small or large, is in any case *finite*. No limit for $N$ tending to infinity will be taken, for this would prevent one from dealing at the same time, and within the same mathematical framework, with discrete, continuous, and hybrid representations. This is a significant difference between our point of view and other approaches, based on similar ideas, that have been used in the literature for bridging models at different scales in the limit $N \to \infty$, see e.g., [6, 7, 20].

## A.1 Cell-based microscopic dynamics

In Section 2 we modeled the positions of the cells in the physical space $\mathbb{R}^d$ at time $t$ as $\mathscr{F}_t$-measurable random variables $\{X_t^i\}_{i=1}^N$, defined on the stochastic basis $(\Omega,\, \mathscr{F},\, (\mathscr{F}_t)_t,\, P)$, with values in the measurable space $(\mathbb{R}^d,\, \mathscr{B}(\mathbb{R}^d))$. We assume now, in more detail, that $(X_t^i)_{t\in[0,\,T_{\max}]}$ is, for all $i$, a continuous-in-time process obeying some stochastic evolution equation. A prototype for chemical-induced taxis and binary interaction-based dynamics is

$$dX_t^i = \left(\mathcal{T}[c_t](X_t^i) + \sum_{j=1}^N K(X_t^i,\, X_t^j)\right) dt + \sqrt{2\sigma}\, dW_t^i, \quad i = 1,\, \dots,\, N, \tag{26}$$

where $\sigma \geq 0$ is a constant (in the simplest case) and $(W_t^i)_{t\in[0,\,T_{\max}]}$ are independent standard Wiener processes modeling stochastic fluctuations in cell motion (i.e., they summarize all aspects of cell behavior on which there is no direct phenomenological control).

A few remarks about Eq. (26) are in order.

- It describes the system from a microscopic Lagrangian point of view. In fact, cells are modeled individually and their paths $t \mapsto X_t^i(\omega)$, $\omega \in \Omega$, corresponding to different realizations of the stochastic processes $\{X_t^i\}_{i=1}^N$, are trackable in the physical space $\mathbb{R}^d$.

- It models cell dynamics by controlling directly the velocity rather than the acceleration. This is consistent with the *active* behavior of cells, which, as mentioned in Section 2, are able to express strategies rather than being passively subject to inertia.
- It assumes deterministic cell-cell interactions, in fact the latter are included in the deterministic part of the right-hand side. This is reasonable for applications in which a standard (say, "rational") behavior of individual cells can be identified, over which very large deviations are not expected.

## A.2 Ensemble representation by probability distributions

We now pass to an Eulerian representation of the spatial distribution of the cells by means of probability measures. For this, let us pick a function $\psi \in C_c^\infty(\mathbb{R}^d)$ and compute it along the trajectories of system (26). From Itô's calculus it follows $d\psi(X_t^i) = \nabla\psi(X_t^i) \cdot dX_t^i + \sigma\Delta\psi(X_t^i)\,dt$, whence

$$\begin{aligned}\psi(X_t^i) = \psi(X_0^i) &+ \int_0^t \nabla\psi(X_s^i) \cdot \mathcal{T}[c_t](X_s^i)\,ds + \sum_{j=1}^N \int_0^t \nabla\psi(X_s^i) \cdot K(X_s^i,\, X_s^j)\,ds \\ &+ \sigma \int_0^t \Delta\psi(X_s^i)\,ds + \sqrt{2\sigma} \int_0^t \nabla\psi(X_s^i) \cdot dW_s^i\end{aligned}$$

for all $t \in [0,\, T_{\max}]$. Taking the expectation of both sides and interchanging properly the order of integration at the right-hand side by Fubini's Theorem gives

$$\begin{aligned}\int_\Omega \psi(X_t^i(\omega))\,dP(\omega) = \int_\Omega \psi(X_0^i(\omega))\,dP(\omega) &+ \int_0^t \int_\Omega \nabla\psi(X_s^i(\omega)) \cdot \mathcal{T}[c_t](X_s^i(\omega))\,dP(\omega)\,ds \\ &+ \sum_{j=1}^N \int_0^t \int_\Omega \nabla\psi(X_s^i(\omega)) \cdot K(X_s^i(\omega),\, X_s^j(\omega))\,dP(\omega)\,ds \\ &+ \sigma \int_0^t \int_\Omega \Delta\psi(X_s^i(\omega))\,dP(\omega)\,ds.\end{aligned}$$

Particularly, we notice that $\mathbb{E}[\int_0^t \nabla\psi(X_s^i) \cdot dW_s^i] = 0$ for all $t \in [0,\, T_{\max}]$ due to the properties of Itô's stochastic integral.

Let now $\mu_t^i = X_t^i \# P \in \mathscr{P}(\mathbb{R}^d)$ be the law of $X_t^i$ and $\mu_t^{ij} = (X_t^i,\, X_t^j)\#P \in \mathscr{P}(\mathbb{R}^d \times \mathbb{R}^d)$ the joint law of $X_t^i,\, X_t^j$. The previous formula can be rewritten as

$$\begin{aligned}\int_{\mathbb{R}^d} \psi(x)\,d\mu_t^i(x) = \int_{\mathbb{R}^d} \psi(x)\,d\mu_0^i(x) &+ \int_0^t \int_{\mathbb{R}^d} \nabla\psi(x) \cdot \mathcal{T}[c_t](x)\,d\mu_s^i(x)\,ds \\ &+ \sum_{j=1}^N \int_0^t \int_{\mathbb{R}^d \times \mathbb{R}^d} \nabla\psi(x) \cdot K(x,\, y)\,d\mu_s^{ij}(x,\, y)\,ds + \sigma \int_0^t \int_{\mathbb{R}^d} \Delta\psi(x)\,d\mu_s^i(x)\,ds.\end{aligned} \tag{27}$$

In order to proceed toward an equation for the marginal distribution $\mu_t^i$, we disintegrate $\mu_t^{ij}$ on $\mathbb{R}^d \times \mathbb{R}^d$ using the canonical projection $\pi : \mathbb{R}^d \times \mathbb{R}^d \to \mathbb{R}^d$, $\pi(x,\, y) = x$. Notice that $\mu_t^i = \pi \# \mu_t^{ij}$ by definition and that, for all $x \in \mathbb{R}^d$, the set $\pi^{-1}(\{x\}) \subset \mathbb{R}^d \times \mathbb{R}^d$ can be identified with $\mathbb{R}^d$ itself. Hence, owing to the disintegration theorem [1], for all $t > 0$ and all $j = 1,\, \dots,\, N$ there exists a family of probability measures $\{\mu_t^{j|i}(\cdot|x)\}_{x \in \mathbb{R}^d} \subset \mathscr{P}(\mathbb{R}^d \times \mathbb{R}^d)$, parameterized by $x$, such that:

- $\mu_t^{j|i}(\cdot|x)$ is unique for $\mu_t^i$-a.e. $x \in \mathbb{R}^d$;
- $\operatorname{supp} \mu_t^{j|i}(\cdot|x) \subseteq \pi^{-1}(\{x\}) \sim \mathbb{R}^d$ for $\mu_t^i$-a.e. $x \in \mathbb{R}^d$;
- $\mu_t^{ij}(dxdy) = \mu_t^{j|i}(dy|x) \otimes \mu_t^i(dx)$ for $\mu_t^{ij}$-a.e. $(x,\, y) \in \mathbb{R}^d \times \mathbb{R}^d$.

We notice that the second condition means that $\mu_t^{j|i}(\cdot|x)$ "lives" actually on $\mathbb{R}^d$ and can therefore be identified with an element of $\mathscr{P}(\mathbb{R}^d)$. The third one is instead a restatement of the conditional probability theorem, up to understanding $\mu_t^{j|i}(\cdot|x)$ as the distribution of $X_t^j$ conditioned to $X_t^i$. Particularly, it implies that integrals on $\mathbb{R}^d \times \mathbb{R}^d$ can be computed as iterated integrals on $\mathbb{R}^d$, thus we have:

$$\int\limits_{\mathbb{R}^d \times \mathbb{R}^d} \nabla\psi(x) \cdot K(x,\, y)\, d\mu_s^{ij}(x,\, y) = \int\limits_{\mathbb{R}^d} \nabla\psi(x) \cdot \left( \int\limits_{\mathbb{R}^d} K(x,\, y)\, d\mu_s^{j|i}(y|x) \right) d\mu_s^i(x).$$

Consequently, Eq. (27) becomes

$$\begin{aligned} \int\limits_{\mathbb{R}^d} \psi(x)\, d\mu_t^i(x) = & \int\limits_{\mathbb{R}^d} \psi(x)\, d\mu_0^i(x) \\ & + \int\limits_0^t \int\limits_{\mathbb{R}^d} \nabla\psi(x) \cdot \left( \mathcal{T}[c_t](x) + \sum_{j=1}^N \int\limits_{\mathbb{R}^d} K(x,\, y)\, d\mu_s^{j|i}(y|x) \right) d\mu_s^i(x)\, ds \\ & + \sigma \int\limits_0^t \int\limits_{\mathbb{R}^d} \Delta\psi(x)\, d\mu_s^i(x)\, ds \end{aligned}$$

or, defining the velocity field

$$v_t^i(x) := \mathcal{T}[c_t](x) + \sum_{j=1}^N \int\limits_{\mathbb{R}^d} K(x,\, y)\, d\mu_t^{j|i}(y|x) \tag{28}$$

and denoting by $\langle \cdot,\, \cdot \rangle$ the duality pairing between distributions and test functions in $C_c^\infty(\mathbb{R}^d)$,

$$\frac{d}{dt}\langle \mu_t^i,\, \psi \rangle + \langle \nabla \cdot (\mu_t^i v_t^i),\, \psi \rangle = \sigma \langle \Delta\mu_t^i,\, \psi \rangle, \quad \forall\, \psi \in C_c^\infty(\mathbb{R}^d), \text{ a.e. } t \in (0,\, T_{\max}]$$

which is the functional form of the following advection-diffusion equation:

$$\frac{\partial \mu_t^i}{\partial t} + \nabla \cdot (\mu_t^i v_t^i) = \sigma \Delta \mu_t^i. \tag{29}$$

Equations (28), (29) provide a deterministic Eulerian representation of the cell colony with cell trajectories $t \mapsto X_t^i(\omega)$ blurred into the spatiotemporal evolution of the probability distribution of cell positions in $\mathbb{R}^d$.

## A.3 Toward a self-contained modeling framework

We discuss now a few manipulations that allow one to recover model (2)-(4) out of the general structure delivered by Eqs. (28), (29), and we critically analyze their validity and significance for modeling.

We recall that in Section 2 we made the further assumption that cells are indistinguishable. In the present context this corresponds to the ansatz $\mu_t^1 = \cdots = \mu_t^N$ on the solutions to Eq. (29), which, for coherence, calls for the ansatz that also the conditioned law $\mu_t^{j|i}(\cdot|x)$ does not depend on the specific pair of indexes $(i,\, j)$. Let $\mu_t$ be the common law of the $X_t^i$'s and $\mu_t(\cdot|x)$ their pairwise joint law. Equation (28) takes the form

$$v_t(x) = \mathcal{T}[c_t](x) + N \int\limits_{\mathbb{R}^d} K(x,\, y)\, d\mu_t(y|x), \tag{30}$$

while Eq. (29) specializes in Eq. (2) up to technically setting $\sigma = 0$ (namely, disregarding the effect of random walks of the cells).

With the further approximation $\mu_t(\cdot|x) \sim \mu_t$ for $\mu_t$-a.e. $x \in \mathbb{R}^d$, Eq. (30) becomes exactly the velocity field (4). We point out that the correct way of understanding such an approximation is in terms of the Wasserstein distance between $\mu_t(\cdot|x)$ and $\mu_t$ in the space of probability measures with finite first moment. Indeed, it is this metric that is the most suited for model (2)-(4), cf. [21]. We also observe that the accuracy of this approximation may depend, among other things, on:

- the assumed microscopic dynamics of the interactions, namely on the specific choice of $K$ (for instance, if $K \equiv 0$ then the approximation is actually exact);
- the total number of cells in the population. Heuristically, the larger $N$ the lower the expected statistical dependence between single pairs of cells, because the dynamics of a cell are presumably affected by many other neighboring cells.

More accurate approximations, involving the assessment of the correlation between pairs of interacting cells, may be envisaged, adapting to the present context some arguments proposed for similar issues in different fields (cf. e.g., [16] about vehicular traffic).

From a different point of view, replacing $\mu_t(\cdot|x)$ with $\mu_t$ in Eq. (30) can be interpreted as a further modeling of the interactions among cells, that would be technically more difficult to implement in an individual-based framework. In more detail, it implies that the interaction strategy of the test cell does not depend on the past history: at each time, it reacts at field cells as if they had just been scattered randomly and independently in the surrounding space. Such a behavior can be justified in view of the indistinguishability of cells and of the non-cooperativeness of their dynamics (i.e., there is no jointly organized strategy among them). Detailing such an effect in Eq. (26) is perhaps not immediate and, after all, also needless, since the final interest is in the Eulerian framework (28)-(29).

Finally, it is worth noticing that, in the case of a purely discrete representation of the cell population, the replacement of $\mu_t(\cdot|x)$ with $\mu_t$ is fully consistent with Eq. (26). Indeed, if $\mu_t$ is given by Eq. (8) then the velocity (4), evaluated at the $h$-th atom of $\mu_t$, coincides with the deterministic part of Eq. (26).

# References

[1] L. Ambrosio, N. Gigli, and G. Savaré. *Gradient flows in metric spaces and in the space of probability measures.* Lectures in Mathematics ETH Zürich. Birkhäuser Verlag, Basel, second edition, 2008.

[2] N. J. Armstrong, K. J. Painter, and J. A. Sherratt. A continuum approach to modelling cell-cell adhesion. *J. Theoret. Biol.*, 243(1):98–113, 2006.

[3] N. J. Armstrong, K. J. Painter, and J. A. Sherratt. Adding adhesion to a chemical signaling model for somite formation. *Bull. Math. Biol.*, 71(1):1–24, 2009.

[4] M. Bertsch, M. E. Gurtin, D. Hilhorst, and L. A. Peletier. On interacting populations that disperse to avoid crowding: The effect of a sedentary colony. *J. Math. Biol.*, 19(1):1–12, 1984.

[5] M. Bertsch, M. E. Gurtin, D. Hilhorst, and L. A. Peletier. On interacting populations that disperse to avoid crowding: preservation of segregation. *J. Math. Biol.*, 23(1):1–13, 1985.

[6] M. Bodnar and J. J. L. Velazquez. Derivation of macroscopic equations for individual cell-based models: a formal approach. *Math. Methods Appl. Sci.*, 28(15):1757–1779, 2005.

[7] V. Capasso and D. Morale. Asymptotic behavior of a system of stochastic particles subject to nonlocal interactions. *Stoch. Anal. Appl.*, 27(3):574–603, 2009.

[8] V. Capasso and D. Morale. Stochastic modelling of tumour-induced angiogenesis. *J. Math. Biol.*, 58(1-2):219–233, 2009.

[9] M. A. J. Chaplain, M. Lachowicz, Z. Szymańska, and D. Wrzosek. Mathematical modelling of cancer invasion: the importance of cell-cell adhesion and cell-matrix adhesion. *Math. Models Methods Appl. Sci.*, 21(4):719–743, 2011.

[10] E. Cristiani, P. Frasca, and B. Piccoli. Effects of anisotropic interactions on the structure of animal groups. *J. Math. Biol.*, 62(4):569–588, 2011.

[11] E. Cristiani, B. Piccoli, and A. Tosin. Modeling self-organization in pedestrians and animal groups from macroscopic and microscopic viewpoints. In G. Naldi, L. Pareschi, and G. Toscani, editors, *Mathematical Modeling of Collective Behavior in Socio-Economic and Life Sciences*, Modeling and Simulation in Science, Engineering and Technology, pages 337–364. Birkhäuser, Boston, 2010.

[12] E. Cristiani, B. Piccoli, and A. Tosin. Multiscale modeling of granular flows with application to crowd dynamics. *Multiscale Model. Simul.*, 9(1):155–182, 2011.

[13] D. Drasdo. Coarse graining in simulated cell populations. *Adv. Complex Syst.*, 8(2–3):319–363, 2005.

[14] T. Hillen, K. Painter, and C. Schmeiser. Global existence for chemotaxis with finite sampling radius. *Discrete Contin. Dyn. Syst. Ser. B*, 7(1):125–144, 2007.

[15] P. Macklin, M. E. Edgerton, A. Thompson, and V. Cristini. Patient-calibrated agent-based modelling of ductal carcinoma in situ (DCIS) I: Model formulation and analysis. *J. Theoret. Biol.*, 2011. (Accepted pending revision).

[16] P. Nelson. A kinetic model of vehicular traffic and its associated bimodal equilibrium solutions. *Transport Theor. Stat.*, 24(1-3):383–409, 1995.

[17] K. J. Painter, N. J. Armstrong, and J. A. Sherratt. The impact of adhesion on cellular invasion processes in cancer and development. *J. Theoret. Biol.*, 264(3):1057–1067, 2010.

[18] B. Piccoli and A. Tosin. Time-evolving measures and macroscopic modeling of pedestrian flow. *Arch. Ration. Mech. Anal.*, 199(3):707–738, 2011.

[19] M. Scianna, L. Munaron, and L. Preziosi. A multiscale hybrid approach for vasculogenesis and related potential blocking therapies. *Prog. Biophys. Mol. Biol.*, 2011. In press (`doi: 10.1016/j.pbiomolbio.2011.01.004`).

[20] A. Stevens. The derivation of chemotaxis equations as limit dynamics of moderately interacting stochastic many-particle systems. *SIAM J. Appl. Math.*, 61(1):183–212, 2000.

[21] A. Tosin and P. Frasca. Existence and approximation of probability measure solutions to models of collective behaviors. *Netw. Heterog. Media*, 2011. In press (`arXiv:1012.2395`).

[22] S. M. Wise, J. S. Lowengrub, H. B. Frieboes, and V. Cristini. Three-dimensional multispecies nonlinear tumor growth – I: Model and numerical method. *J. Theoret. Biol.*, 253(3):524–543, 2008.

[23] T. P. Witelski. Segregation and mixing in degenerate diffusion in population dynamics. *J. Math. Biol.*, 35(6):695–712, 1997.